0026-895X/03/6405-1136–1144$7.00
MOLECULAR PHARMACOLOGY
Copyright © 2003 The American Society for Pharmacology and Experimental Therapeutics
Mol Pharmacol 64:1136–1144, 2003

Vol. 64, No. 5
2737/1103450
Printed in U.S.A.

Effect of Glutathione Depletion on Sites and Topology of Superoxide and Hydrogen Peroxide Production in Mitochondria

DERICK HAN, RAFFAELLA CANALI, DANIEL RETTORI, and NEIL KAPLOWITZ

USC-UCLA Research Center for Alcoholic and Pancreatic Disease, University of Southern California Research Center for Liver Diseases, Keck School of Medicine (D.H., N.K.), and Department of Molecular Pharmacology & Toxicology, School of Pharmacy (R.C. D.R.), University of Southern California, Los Angeles, California

Received June 12, 2003; accepted August 4, 2003

This article is available online at http://molpharm.aspetjournals.org

ABSTRACT

In this work, the topology of mitochondrial $O_2^{\cdot-}$ and H_2O_2 generation and their interplay with matrix GSH in isolated heart mitochondria were examined. We observed that complex I releases $O_2^{\cdot-}$ into the matrix (where it is converted to H_2O_2 by Mn-SOD) but not into the intermembrane space. No free radical generation was observed from complex II, but succinate treatment caused H_2O_2 generation from the matrix through a reverse electron flow to complex I. Complex III was found to release $O_2^{\cdot-}$ into the matrix and into the intermembrane space. Antimycin, which increases steady-state levels of $UQ_O^{\cdot-}$ (ubisemiquinone at the Qo site) in complex III, enhanced both H_2O_2 generation from the matrix and $O_2^{\cdot-}$ production from the intermembrane space. On the other hand, myxothiazol, which inhibits $UQ_O^{\cdot-}$ formation, completely inhibited antimycin induced $O_2^{\cdot-}$ toward the intermembrane space and inhibited H_2O_2 generation from the matrix by 70%. However, myxothiazol alone enhanced H_2O_2 production from complex III, suggesting that other components of complex III besides the $UQ_O^{\cdot-}$ can cause $O_2^{\cdot-}$ generation toward the matrix. As expected, mitochondrial GSH was found to modulate H_2O_2 production from the matrix but not $O_2^{\cdot-}$ generation from the intermembrane space. Low levels of GSH depletion (from 0–40%, depending on the rate of H_2O_2 production) had no effect on H_2O_2 diffusion from mitochondria. Once this GSH depletion threshold was reached, GSH loss corresponded to a linear increase in H_2O_2 production by mitochondria. The impact of 50% mitochondrial GSH depletion, as seen in certain pathological conditions in vivo, on H_2O_2 production by mitochondria depends on the metabolic state of mitochondria, which governs its rate of H_2O_2 production. The greater the rate of H_2O_2 generation the greater the effect 50% GSH depletion had on enhancing H_2O_2 production.

Glutathione (GSH) is the major nonprotein thiol in cells and plays a key role in detoxification of reactive oxygen metabolites (peroxides) and reactive electrophilic compounds (DeLeve and Kaplowitz, 1991). There exist two major GSH pools in cells, a cytoplasmic and mitochondrial pool; the latter is important in detoxification of H_2O_2 produced by the electron transport chain (Chance et al., 1979). Mitochondrial GSH is considered vital for cell survival. Cell necrosis caused by GSH-depleting agents (e.g., diethylmaleate, acetaminophen) is believed to occur only after severe mitochondrial GSH depletion (greater than 80%), with cytoplasmic GSH depletion being less consequential (Uhlig and Wendel, 1992; Garcia-Ruiz et al., 1995). Cell necrosis after mitochondrial GSH depletion has been ascribed to increased steady-state levels of reactive oxygen species that lead to mitochondria damage and dysfunction (Garcia-Ruiz et al., 1995). In support of this argument is the observation that antioxidant treatment, particularly Vitamin E, is effective in inhibiting or delaying cell necrosis induced by GSH depletion (Han et al., 1997; Nagai et al., 2002).

Mitochondrial GSH depletion occurs in several pathological conditions, including long-term ethanol intake (Fernandez-Checa et al., 1987; Hirano et al., 1992), cerebral ischemia (Anderson and Sims, 2002), exposure to environmental toxins, such as cadmium (Nigam et al., 1999), and during liver regeneration (Vendemiale et al., 1995). In rats receiving long-term ethanol treatment, mitochondrial GSH levels were

The study was supported primarily by Project 1 (N.K.) of the USC-UCLA Research Center for Alcoholic Liver and Pancreatic Diseases [National Institute on Alcohol Abuse and Alcoholism (NIAAA) grant P50-AA11199 (to N.K.)]. D.H. was also supported in part by NIAAA-sponsored postdoctoral training grant T32-AA07578. Resources of the Cell Biology Core, USC Research Center for Liver Diseases, supported by National Institute of Diabetes and Digestive and Kidney Diseases grant P30-DK48522, were used for mitochondrial preparations.

ABBREVIATIONS: DMPO, 5,5′-dimethyl-1-pyrroline-*N*-oxide; CDNB, 1-chloro-2,4 dinitrobenzene; RCR, respiratory control ratio; EPR, electron paramagnetic resonance; MOPS, 4-morpholinepropanesulfonic acid; UQ, ubisemiquinone; SOD, superoxide dismutase; HRP, horseradish peroxidase; HPLC, high-performance liquid chromatography.

found to be selectively decreased by up to 65% after 8 weeks of treatment (Fernandez-Checa et al., 1987). These findings lead to an intriguing question: what is the physiological consequence of moderate mitochondrial GSH depletion seen in vivo in these pathological situations? Although in cultured cells, severe GSH depletion results in cell necrosis, moderate mitochondrial GSH depletion is generally not cytotoxic (Nagai et al., 2002) and physiological effects are not always evident (Uhlig and Wendel, 1992). In terms of mitochondrial H_2O_2 production, the present understanding of the GSH peroxidase system predicts that small changes in mitochondrial GSH levels would have little consequence to H_2O_2 release by mitochondria. GSH peroxidase (E-Cys-Se^-) is a selenium-based enzyme that reduces H_2O_2 to water (Flohe et al., 1976):

$$H_2O_2 + \text{E-Cys-Se}^- + H^+ \rightarrow \text{E-Cys-SeOH} + H_2O \quad (1)$$

$$\text{E-Cys-SeOH} + \text{GSH} \rightarrow \text{E-Cys-SeSG} + H_2O \quad (2)$$

$$\text{E-Cys-SeSG} + \text{GSH} \rightarrow \text{E-Cys-Se}^- + \text{GSSG} + H^+ \quad (3)$$

Mitochondria contain high amounts of GSH (5–10 mM), whereas steady-state levels of H_2O_2 in the matrix are believed to be more than 1000-fold lower (Boveris and Cadenas, 1997). Kinetic data suggests that because of this large stoichiometric difference between GSH and H_2O_2 in the matrix, even a 50% decrease in GSH levels may not have a significant impact on H_2O_2 detoxification (Flohe et al., 1976). Theoretically, within this GSH range, these enzymes are fully reduced with their active selenol site, ready to scavenge any H_2O_2 molecule. However, extrapolation of kinetic studies to the in vivo situation may be misleading. If concentrations of H_2O_2 are highly localized in certain areas of the matrix, the large stoichiometric difference between GSH and H_2O_2 would be partially offset. If we take into consideration the compartmentalization of the matrix and the fact that H_2O_2 can diffuse rapidly through membranes, even small decreases in GSH peroxidase kinetics—caused by lower GSH levels—may lead to an increase in H_2O_2 escape from mitochondria. Because a detailed study of the effects of GSH concentration on H_2O_2 production in mitochondria has not been performed, an understanding of the consequences of mitochondrial GSH depletion that occurs in vivo in certain pathological conditions remains incomplete.

The mechanism of H_2O_2 production by mitochondria, on the other hand, has been extensively studied both in physiological and pathological situations such as aging (Chance et al., 1979; Cadenas and Boveris, 1980; Turrens et al., 1985; Hansford et al., 1997). These studies have shown that complexes I and III, ascribed to flavoprotein (Turrens and Boveris, 1980) and ubisemiquinone autoxidation (Boveris and Cadenas, 1975; Cadenas et al., 1977), respectively, are responsible for $O_2^{\cdot-}$ generation by the respiratory chain. Complex I is believed to generate $O_2^{\cdot-}$ into the matrix, where Mn-SOD converts $O_2^{\cdot-}$ into H_2O_2, which in turn is either reduced by GSH peroxidase or diffuses from mitochondria (Chance et al., 1979). In complex III, ubisemiquinone is formed at both the Q_I site that lies near the matrix and at the Q_O site near the intermembrane space (Brandt, 1998). $Ub_O^{\cdot-}$ (ubisemiquinone at the Q_O site) rather than $Ub_I^{\cdot-}$ (ubisemiquinone at the Q_I site) has been the focus of $O_2^{\cdot-}$ generation by complex III (Demin et al., 1998). Recently, we demonstrated that $Ub_O^{\cdot-}$ in complex III generates $O_2^{\cdot-}$ into the intermembrane space (Han et al., 2001), a portion of which diffuses into the cytoplasm through voltage dependent anion channels (Han et al., 2003). Although the topology of $O_2^{\cdot-}$ and H_2O_2 by mitochondria is becoming better understood, several key questions still remain. For example, it is still not completely clear whether complex I or II is also a source of $O_2^{\cdot-}$ in the intermembrane space.

The purpose of this work was to gain further insight on the topology of mitochondrial $O_2^{\cdot-}$ and H_2O_2 production and to study the consequences of intramitochondrial GSH depletion on their production using isolated heart mitochondria.

Materials and Methods

Chemicals and Biochemicals. 5,5′–Dimethyl-1-pyrroline-*N*-oxide (DMPO), 1-chloro-2,4 dinitrobenzene (CDNB), NADP, superoxide dismutase, myxothiazol, glutamate, malate, succinate, Nagarse, antimycin A, catalase, TTFA (thenoyltrifluoroacetone), and rotenone were obtained from Sigma Chemical Co. (St. Louis, MO).

Isolation of Heart Mitochondria. Heart mitochondria were isolated from adult male Wistar rats by differential centrifugation using Nagarse (Cadenas and Boveris, 1980). Rat hearts were excised, washed, and chopped into fine pieces. Chopped hearts were suspended in an isolation buffer consisting of 230 mM mannitol, 70 mM sucrose, 1 mM EDTA, and 5 mM Trizma/HCl buffer, pH 7.4. The chopped heart was treated with Nagarse (1 mg/heart) for 5 min and then homogenized by 10 strong strokes of a loose-fitting Potter-Elvehjem Teflon pestle. The homogenate was centrifuged at 800*g* for 8 min, the pellet removed, and the centrifugation process was repeated. The resulting supernatant was centrifuged at 8000*g* for 10 min, washed with isolation buffer and the centrifugation repeated. Isolated mitochondria were resuspended in isolation buffer and placed in ice for the duration of experiment.

Determination of Mitochondria Integrity. To determine the integrity of isolated heart mitochondria, oxygen uptake was measured and the respiratory control ratio (RCR) was determined. RCR was defined as the state 3/state 4 ratio. Oxygen uptake was measured polarographically with a Clark-type electrode (Hansatech, King's Lynn, Norfolk, UK) in respiration buffer containing 230 mM mannitol, 70 mM sucrose, 30 mM Tris-HCl, 5 mM KH_2PO_4, 1 mM EDTA, and 0.1% bovine serum albumin, pH 7.4. For all experiments, mitochondria with an RCR greater than 4 using glutamate/malate as substrates were used.

Depeletion of Mitochondrial Glutathione. Mitochondrial GSH was depleted using CDNB, a favored substrate for glutathione transferases localized in the mitochondrial matrix (Jocelyn and Cronshaw, 1985). Glutathione transferase catalyzes the specific conjugation of GSH with CDNB. GSH was depleted using CDNB as follows: isolated mitochondria (5 mg/ml) suspended in isolation buffer were incubated with various concentrations of CDNB dissolved in ethanol for 2 min at room temperature. The pellets were spun at 8000*g* for 5 min and washed once more in isolation buffer. Control mitochondria were treated with an equal amount of ethanol. Treatment of isolated heart mitochondria (5 mg/ml) with 35 μM CDNB resulted in 90 ± 7% depletion of mitochondrial GSH. No changes in mitochondrial respiration or in the respiratory control ratio were observed with the maximum amount of CDNB used (35 μM), in agreement with previous results (Jocelyn and Cronshaw, 1985).

We find the ratio of nanomoles of CDNB to milligrams of heart mitochondria to be important in determining amount of GSH depletion; for lower amounts of mitochondria, lower concentrations of CDNB must be used. No more than 35 μM CDNB can be used for heart mitochondria (5 mg/ml). Higher levels of CDNB will have secondary effects on complex I and may stimulate H_2O_2 production (Zoccarato et al., 1988, 1990). It is important that samples are

washed carefully to remove excess CDNB as to not affect complex I generation of H_2O_2 (Zoccarato et al., 1988).

Determination of Glutathione. Samples of mitochondria were stored in metaphosphoric acid 2% at −80°C until the analysis. GSH levels were quantified by HPLC, using coulometric electrochemical detector (Harvey et al., 1989). The HPLC conditions were performed using an Alltech C18 column 250 × 4.6 mm and an electrochemical detector ESA Coulochem II. The potential settings were: guard cell, + 0.95 V; electrode 1, +0.45 V. The mobile phase consisted of 50 mM NaH_2PO_4 adjusted to pH 2.7 with phosphoric acid.

Superoxide Determination. Superoxide was determined by electron paramagnetic resonance (EPR) with the spin trap, DMPO. EPR with DMPO measures only $O_2^{\cdot-}$ diffusing from mitochondria through the voltage-dependent anion channel, not $O_2^{\cdot-}$ in the matrix (Han et al., 2003). For EPR measurements, heart mitochondria were placed in buffer consisting of 230 mM mannitol, 70 mM sucrose, 20 mM Tris, and 200 units of catalase, and pH was adjusted to 7.4 with MOPS in the absence or presence of mitochondrial respiratory substrates or inhibitors. DMPO was present at a concentration of 160 mM. EPR spectra were recorded with a Bruker ECS106 spectrometer (operating at X-band) equipped with a cylindrical room temperature cavity operating in TM_{110} mode. Aliquots of samples were promptly transferred to bottom-sealed Pasteur pipettes and measured at room temperature with the following settings: receiver gain, 5×10^5; microwave power, 20 mW; microwave frequency, 9.77 GHz; modulation amplitude, 1 G; time constant, 164-ms scan time, 87 s; scan width, 80 G. The DMPO-OH signal generated from heart mitochondria was quantified by comparison with a TEMPOL standard after double integration of both signals as described previously (Han et al., 2003). All spectra shown are an accumulation of seven scans.

Hydrogen Peroxide Measurements. H_2O_2 production by heart mitochondria was measured by monitoring fluorescence of *p*-hydroxyphenylacetate oxidation in the presence of horseradish peroxidase (Hyslop and Sklar, 1984). Fluorescence measurements (λ_{ex} = 320 nm; λ_{em} = 400 nm) were performed with an LS-5 spectrofluorometer (PerkinElmer Life Sciences, Boston, MA) equipped with a thermal-controlled and magnetic stirring sample compartment. For all measurements, mitochondria were incubated in 230 mM mannitol, 70 mM sucrose, and 20 mM Tris (pH was adjusted to 7.4 with MOPS) at 25°C.

The rates of H_2O_2 production by heart mitochondria in this work are much greater than those we previously reported (Han et al., 2003). In our previous work, we used higher amounts of mitochondria, which interferes with fluorescence and underestimates H_2O_2 production and effect of such inhibitors as myxothiazol.

Determination of Aconitase and Fumarase Activities. For aconitase and fumarase measurements, control and GSH depleted mitochondria were treated with glutamate/malate, and at indicated times, mitochondria were spun down (8,000*g* for 8 min). The pellets were stored at −80° until time of analysis. Mitochondria pellets were resuspended in 0.5% Triton X-100 to disrupt the membranes.

Aconitase activity was assayed by following the formation of NADPH at an absorbance of 340 nm at 25°C. The reaction mixture was composed of 30 mM Tris-HCl, pH 7.4, 30 mM sodium citrate, 0.6 mM $MnCl_2$, 0.2 mM $NADP^+$, 1 U/ml of isocitrate dehydrogenase, and 0.1 mg of mitochondria (Gardner and White, 1995).

Fumarase activity was assayed spectrometrically by monitoring the increase in absorbance at 240 nm at 25°C. The reaction mixture was composed of 30 mM KH_2PO_4, pH 7.4, 0.01 mM ETDA, and 5 mM malate (Gardner and White, 1995).

Data Analysis. Statistical analysis was performed using paired *t* test, with the minimum level of significance defined at $p < 0.05$. Where appropriate, means ± S.D. are presented in the text.

Results

Dose-Dependent Depletion of Mitochondrial GSH by CDNB. GSH forms a conjugate with CDNB in the mitochondrial matrix, a process believed to be catalyzed by GSH *S*-transferase (Jocelyn and Cronshaw, 1985). The addition of CDNB to isolated heart mitochondria caused a dose-dependent loss of GSH from the matrix (Fig. 1). CDNB treatment caused no measurable changes in mitochondria; parameters checked included state III and IV respiration and $O_2^{\cdot-}$ generation from complex I (data not shown). Previous studies have reported that high levels of CDNB (60 μM) can induce $O_2^{\cdot-}$ generation from complex I, a phenomenon that can be prevented by washing CDNB out of mitochondria (Zoccarato et al., 1988), as done in this work.

H_2O_2 Production Using Complex I Substrates: Effect of GSH Depletion. To assess H_2O_2 production by complex I, mitochondria were treated with complex I substrates (glutamate/malate), and kinetics of H_2O_2 production was monitored fluorometrically in the presence of *p*-hydroxyphenylacetate and horseradish peroxidase. The complex I inhibitor rotenone was also added to mitochondria to observe the effect of inhibition of complex I on H_2O_2 production. The consequences of GSH depletion (90 ± 7%) on H_2O_2 production using glutamate/malate as substrates are summarized in Table 1. Rotenone was effective in causing a large increase in H_2O_2 production in both control and GSH-depleted mitochondria. It is believed that rotenone blockage of complex I allows for greater flavoprotein autoxidation (Turrens and Boveris, 1980).

A dose-dependent relationship between GSH depletion and H_2O_2 production in the presence of glutamate/malate and rotenone is shown in Fig. 2. A biphasic curve is observed—the first phase, in which GSH depletion has no effect on H_2O_2 production, is followed by a second phase, in which GSH depletion is linearly related to increases in H_2O_2 production. These data show that a certain threshold of GSH depletion must be reached before H_2O_2 diffusion from the mitochondrial matrix increases.

H_2O_2 Production Using Complex II Substrate: Effect of GSH Depletion. The addition of the complex II substrate succinate to heart mitochondria also caused dramatic increases in H_2O_2, an effect that was curtailed by rotenone

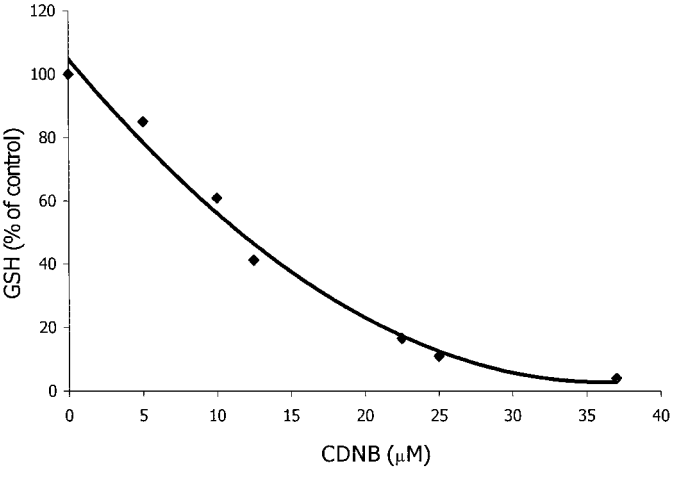

Fig. 1. Dose-dependent depletion of GSH by CDNB in isolated heart mitochondria. Isolated mitochondria (5 mg/ml), suspended in isolation buffer, were incubated with various concentrations of CDNB dissolved in ethanol for 2 min at room temperature. The pellets were spun at 8000*g* for 5 min and washed once more in isolation buffer. Control mitochondria were treated with the same amount of ethanol. GSH was determined by HPLC using electrochemical detection.

treatment (Table 1). GSH-depleted (90 ± 7%) mitochondria exhibited an increase of more than 2-fold in H_2O_2 production compared with control. The fact that rotenone, a complex I inhibitor, decreased H_2O_2 production by a complex II substrate suggests that a reversal of electron flow was occurring, with H_2O_2 production resulting from oxidation of the flavoprotein in complex I (Turrens and Boveris, 1980; Hensley et al., 1998). This reversed electron flow in the presence of succinate has been observed in other systems and represents another pathway of H_2O_2 production by complex I. The addition of the complex II inhibitor, TTFA, resulted in complete elimination of H_2O_2 production by mitochondria. The effect of TTFA is in agreement with previous observations (Cadenas and Boveris, 1980) and supports the notion that inhibition of complex II does not induce $O_2^{\cdot-}$ generation.

Decreasing mitochondrial GSH levels also resulted in increased H_2O_2 production in mitochondria treated with succinate (Fig. 3). The GSH-H_2O_2 dose curve with succinate treatment was biphasic, similar to the GSH-H_2O_2 dose curve observed with glutamate/malate plus rotenone treatment. The GSH-H_2O_2 dose curve with succinate had a slightly lower threshold of GSH depletion (~27%) needed before H_2O_2 production increased, compared with the threshold observed with glutamate/malate plus rotenone (~37%). The fact that succinate treatment was associated with higher H_2O_2 generation suggests that the threshold of GSH depletion needed before increased H_2O_2 production may vary according to the rate of H_2O_2 production.

Effect of 50% Mitochondrial GSH Depletion on H_2O_2 Production by Mitochondria. The effect of 50% mitochondrial GSH depletion, as seen in vivo in certain pathological conditions such as ethanol exposure (Fernandez-Checa et al., 1987), on mitochondrial H_2O_2 production was analyzed. Figure 4 shows that the greater the rate of H_2O_2 production, the more 50% GSH depletion enhanced H_2O_2 generation in heart

TABLE 1

Effect of GSH depletion on mitochondrial H_2O_2 production

Control and GSH depleted (90 ± 7%) heart mitochondria (0.08 mg) were incubated in a buffer containing 230 mM mannitol, 70 mM sucrose, 20 mM Tris-HCl (pH adjusted to 7.4 with MOPS) at 25°C with HRP (10 U) and *p*-hydroxyphenylacetate (1 mM). When present, glutamate/malate = 7.5 mM, succinate = 7.5 mM, TTFA = 20 μM, and rotenone = 2 μM. <0.02 represents the detection limit of the method. Data are presented as mean ± S.D.

	H_2O_2	
	Control	GSH-Depleted
	nmol/min/mg	
Complex I substrate		
Glutamate/malate	<0.02	0.058 ± 0.049
Glutamate/malate plus rotenone	0.15 ± 0.045	0.42 ± 0.15*
Complex II substrate		
Succinate	1.15 ± 0.51	2.43 ± 0.97*
Succinate plus TTFA	<0.02	<0.02
Succinate plus rotenone	0.053 ± 0.05	0.097 ± 0.88

TTFA, 4,4,4-trifluoro-1-(2-thienyl)-1,3-butanedione.
* $P < 0.05$ compared with control.

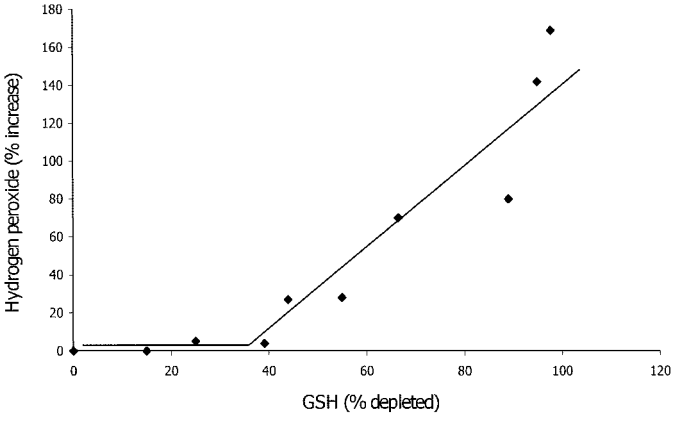

Fig. 2. Dose-dependent effect of GSH depletion on H_2O_2 production by complex I. GSH was depleted in isolated heart mitochondria using various concentrations of CDNB. Mitochondria were treated with glutamate/malate plus rotenone, and H_2O_2 production was monitored using HRP (10 U) and *p*-hydroxyphenylacetate (1 mM) in buffer [230 mM mannitol, 70 mM sucrose, and 20 mM Tris/HCl (pH adjusted to 7.4 with MOPS)] at 25°C.

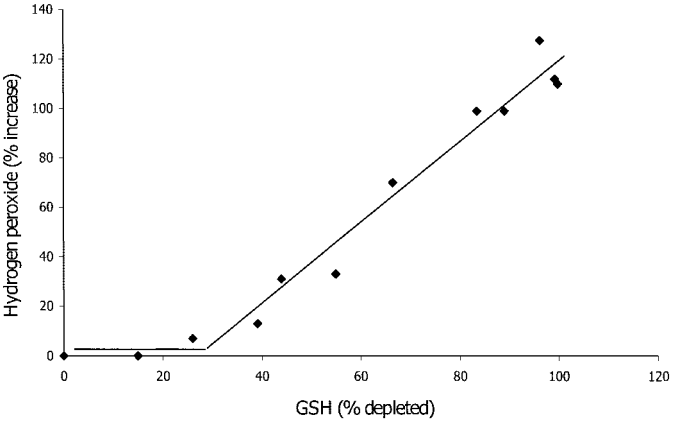

Fig. 3. Dose-dependent effect of GSH depletion on H_2O_2 production in the presence of succinate. GSH was depleted in isolated heart mitochondria using various concentration of CDNB. Mitochondria were treated with succinate and H_2O_2 production was monitored using HRP (10 U) and *p*-hydroxyphenylacetate (1 mM) in buffer at 25°C.

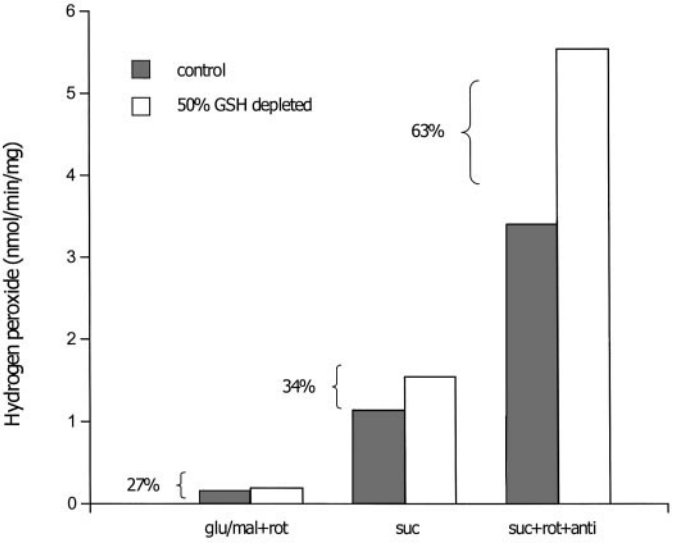

Fig. 4. Effect of 50% mitochondrial GSH depletion on H_2O_2 production by mitochondria. The rates of H_2O_2 production were compared in control and 50% GSH-depleted mitochondria. The values noted in the figure represent the percentage increase as a consequence of 50% GSH depletion. The succinate plus rotenone plus antimycin-treated values represent measurements of short, high bursts of H_2O_2 that occur in mitochondria after antimycin treatment. Heart mitochondria (0.08 mg) were incubated in a buffer containing 230 mM mannitol, 70 mM sucrose, 20 mM Tris/HCl (pH adjusted to 7.4 with MOPS) at 25°C with HRP (10 U) and *p*-hydroxyphenylacetate (1 mM). When present, succinate = 7.5 mM, and rotenone = 2 μM. *, $P < 0.05$ compared with control.

mitochondria. The succinate plus rotenone plus antimycin-treated values represent measurements of short, high bursts of H_2O_2 that occur after antimycin treatment. In presence of glutamate/malate (a very low range of H_2O_2 production, 0.010 ± 0.008 nmol/min/mg), 50% GSH depletion had no affect on H_2O_2 production (data not shown). Mitochondria treated with glutamate/malate may not have had enhanced H_2O_2 production with 50% GSH depletion because it may not have reached the threshold of GSH depletion needed to affect H_2O_2 levels. However, it must be noted that small changes in H_2O_2 levels are difficult to measure when H_2O_2 production rates are so low as with mitochondria treated with glutamate/malate.

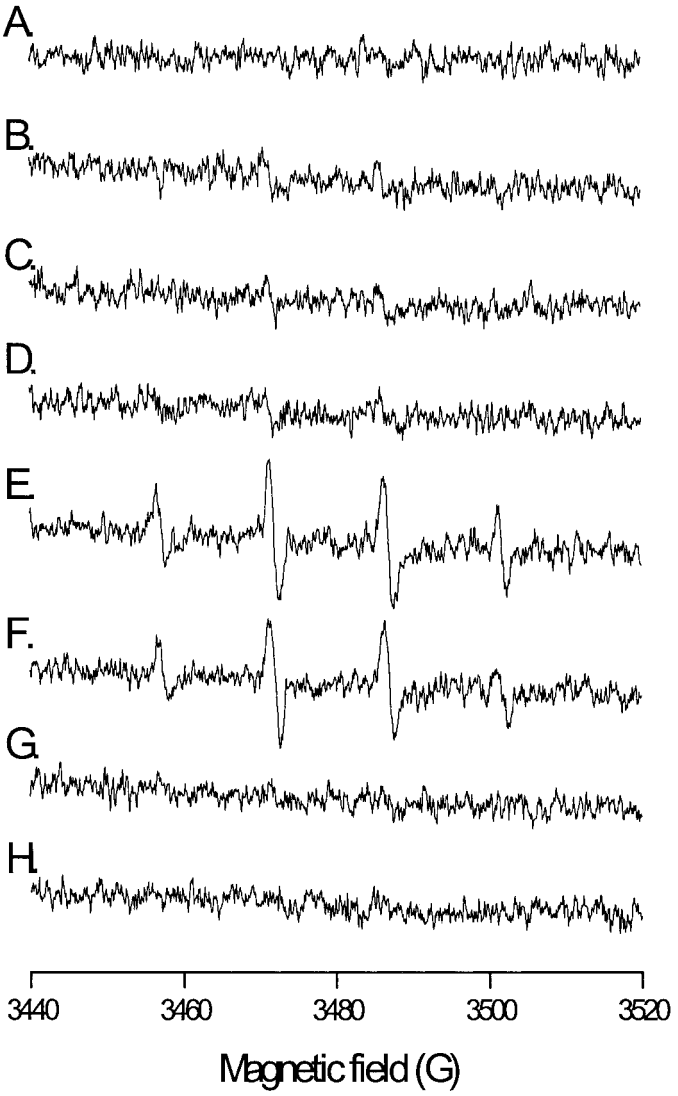

Fig. 5. Superoxide generation by heart mitochondria: effect of inhibitors and GSH depletion. Assay conditions: the reaction mixture consisted of mitochondria (0.04 mg of protein/ml) in buffer (230 mM mannitol/70 mM sucrose/20 mM Tris, and 200 U catalase) pH 7.4, supplemented with 160 mM DMPO and respiratory substrate and/or inhibitor. A, no treatment; B, glutamate/malate; C, succinate plus rotenone; D, glutamate/malate plus rotenone; E, succinate plus rotenone plus antimycin; F, succinate plus rotenone plus antimycin—GSH-depleted mitochondria (by 90%); G, succinate plus rotenone plus antimycin plus myxothiazol; H, succinate plus rotenone plus antimycin plus SOD. When present, glutamate/malate = 7.5 mM; succinate = 7.5 mM; rotenone = 2 μM; SOD = 2 μM; myxothiazol = 2 μM; and antimycin = 1 μg/mg protein.

Superoxide Generation by Heart Mitochondria: Effect of Inhibitors and GSH Depletion. EPR experiments with the spin trap DMPO were performed to examine the topology of $O_2^{\cdot-}$ production in mitochondria and to determine the effect of GSH depletion on $O_2^{\cdot-}$ production. In the absence of respiratory substrates, no observable EPR signal was observed in mitochondria treated with DMPO (Fig. 5A). The addition of complex I (glutamate/malate 10 mM; Fig. 5B) or complex II (succinate 10 mM + rotenone 2 μM; Fig. 5C) substrates to heart mitochondria resulted in a low-intensity EPR signal characteristic of the DMPO-OH spin adduct (quartet signal with intensity ratios of 1:2:2:1; $a^N = a^H = 14.9$). The DMPO-OH signal is formed by spontaneous decay of the DMPO-superoxide adduct (DMPO-OOH) in mitochondria (Finkelstein et al., 1980). Both complex I and complex II substrates induced $O_2^{\cdot-}$ formation, indicating that a low level of $O_2^{\cdot-}$ is generated by complex III. The addition of rotenone in the presence of glutamate/malate caused no substantial increase in $O_2^{\cdot-}$ production (Fig. 5D), suggesting that complex I is not a source of $O_2^{\cdot-}$ into the intermembrane space. The DMPO-OH signal after succinate treatment (data not shown) was similar for mitochondria treated with succinate plus rotenone, suggesting that reverse electron flow did not induce $O_2^{\cdot-}$ generation toward the intermembrane space. The treatment of mitochondria with the complex II inhibitor TTFA and succinate also failed to generate a DMPO-OH signal (data not shown), indicating that complex II is not a source of $O_2^{\cdot-}$ into the intermembrane space.

Antimycin, which inhibits complex III to cause increases in $UQ_O^{\cdot-}$ levels but inhibits $UQ_I^{\cdot-}$ levels (de Vries, 1986), caused an increase of the EPR signal intensity (Fig. 5E) in mitochondria treated with succinate plus rotenone. As expected, no difference in the DMPO-OH signal was observed in control and GSH depleted mitochondria (90 ± 7%) in either succinate plus rotenone-treated mitochondria (data not shown) or mitochondria treated with succinate plus rotenone and antimycin (Fig. 5, E and F). Myxothiazol, a complex III inhibitor that inhibits $UQ_O^{\cdot-}$ formation (de Vries, 1986), was found to abolish the EPR signal generated by antimycin (Fig. 5G). The DMPO-OH signal was confirmed to be $O_2^{\cdot-}$ by the addition of exogenous Cu,Zn-SOD, which abolished the EPR signal generated by mitochondria (Fig. 5H).

Effect of Antimycin and Myxothiazol on $O_2^{\cdot-}$ and H_2O_2 Production by Complex III: Effect of GSH Depletion. The generation of $O_2^{\cdot-}$ and H_2O_2 by complex III and their modulation by GSH was further analyzed. As seen with $O_2^{\cdot-}$, the production of H_2O_2 from complex III can be enhanced by the addition of the antimycin, an effect largely inhibited by myxothiazol (Fig. 6A). However, myxothiazol did not completely inhibit antimycin-induced H_2O_2 generation, and myxothiazol alone induced H_2O_2 generation from mitochondria. This contrasts with mitochondrial $O_2^{\cdot-}$ generation, where myxothiazol treatment alone failed to induce $O_2^{\cdot-}$ generation and almost completely inhibited $O_2^{\cdot-}$ from the intermembrane space (Fig. 6B). Taken together, these results suggest that $UQ_O^{\cdot-}$ induced by antimycin, can release $O_2^{\cdot-}$ both toward the intermembrane space (where it diffuses through voltage dependent anion channels) and toward the matrix (where it is converted to H_2O_2 by Mn-SOD in the matrix). Myxothiazol, by inhibiting $UQ_O^{\cdot-}$ formation, caused a nearly complete inhibition of antimycin-induced $O_2^{\cdot-}$ toward the intermembrane space and inhibited H_2O_2 generation from the matrix by 70%.

The fact that myxothiazol treatment alone enhanced H_2O_2 production from complex III suggests that another component of complex III besides the $UQ_O^{\cdot-}$ contributes to $O_2^{\cdot-}$ generation toward the matrix, in agreement with previous studies (Starkov and Fiskum, 2001; Young et al., 2002). Furthermore, even in the presence of antimycin, it is possible that other components besides $UQ_O^{\cdot-}$ contribute to $O_2^{\cdot-}$ release into the matrix, because H_2O_2 production was higher with antimycin plus myxothiazol (0.43 nmol/min/mg) than with myxothiazol alone (0.28 nmol/min/mg) (Fig. 6A).

The depletion of GSH (90 ± 7%) resulted in an 83% increase in H_2O_2 production by mitochondria in presence of antimycin (Fig. 6A). Myxothiazol in certain cases can inhibit complex I and modulate $O_2^{\cdot-}$ generation, so complex II substrate succinate plus complex I inhibitor rotenone were used in these experiments.

Effect of GSH Depletion on the Activity of Matrix Enzymes Aconitase and Fumarase. To determine the consequences of H_2O_2 production caused by GSH depletion in the

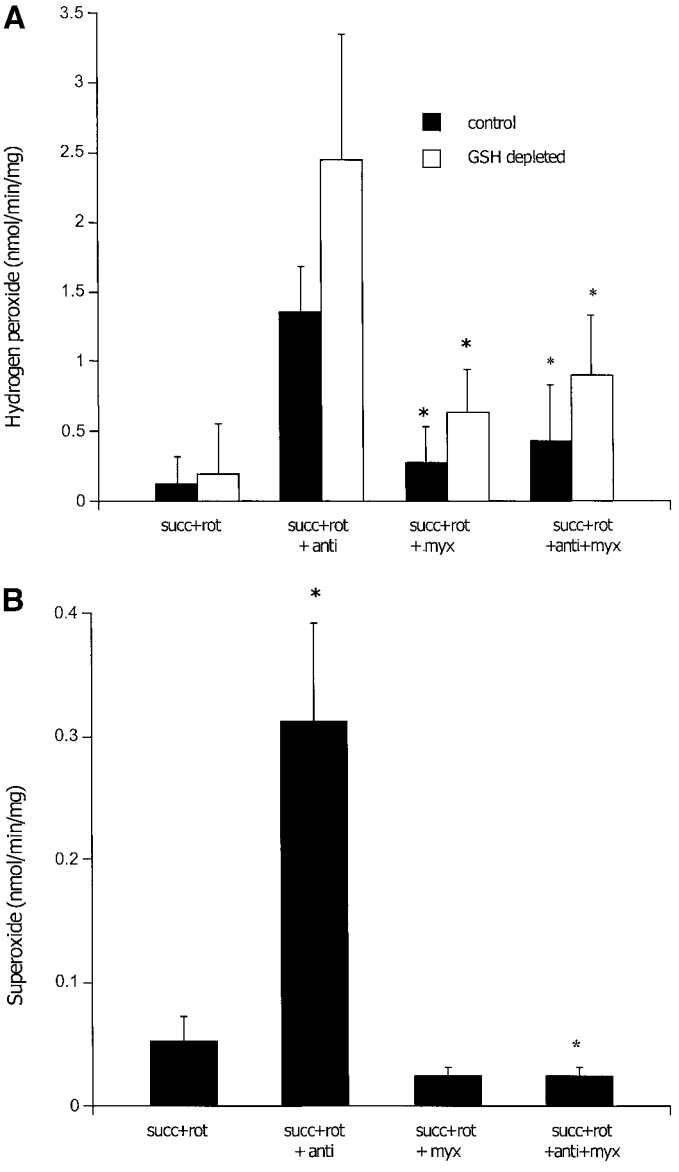

Fig. 6. Effect of antimycin and myxothiazol on $O_2^{\cdot-}$ and H_2O_2 production by complex III: effect of GSH depletion. A, effect of GSH depletion (90 ± 7%), antimycin, and myxothiazol on H_2O_2 production by heart mitochondria in presence of succinate plus rotenone. Heart mitochondria (0.08 mg) were incubated in a buffer containing 230 mM mannitol, 70 mM sucrose, 20 mM Tris/HCl (pH adjusted to 7.4 with MOPS) at 25°C with HRP (10 U) and *p*-hydroxyphenylacetate (1 mM). B, effect of antimycin and myxothiazol on $O_2^{\cdot-}$ production by heart mitochondria in presence of succinate plus rotenone. Assays were carried in buffer (230 mM mannitol/70 mM sucrose/20 mM Tris, and 20 U catalase), pH 7.4, supplemented with 160 mM DMPO using 0.04 mg of protein/ml of mitochondria. $O_2^{\cdot-}$ levels were estimated using TEMPOL as standard. When present, succinate (succ) = 7.5 mM, rotenone (rot) = 2 μM, myxothiazol (myx) = 2 μM, and antimycin (anti) = 1 μg/mg protein. ⋆, $P < 0.05$ compared with control. ⋆, $P < 0.05$ compared with mitochondria treated with succinate plus rotenone plus antimycin.

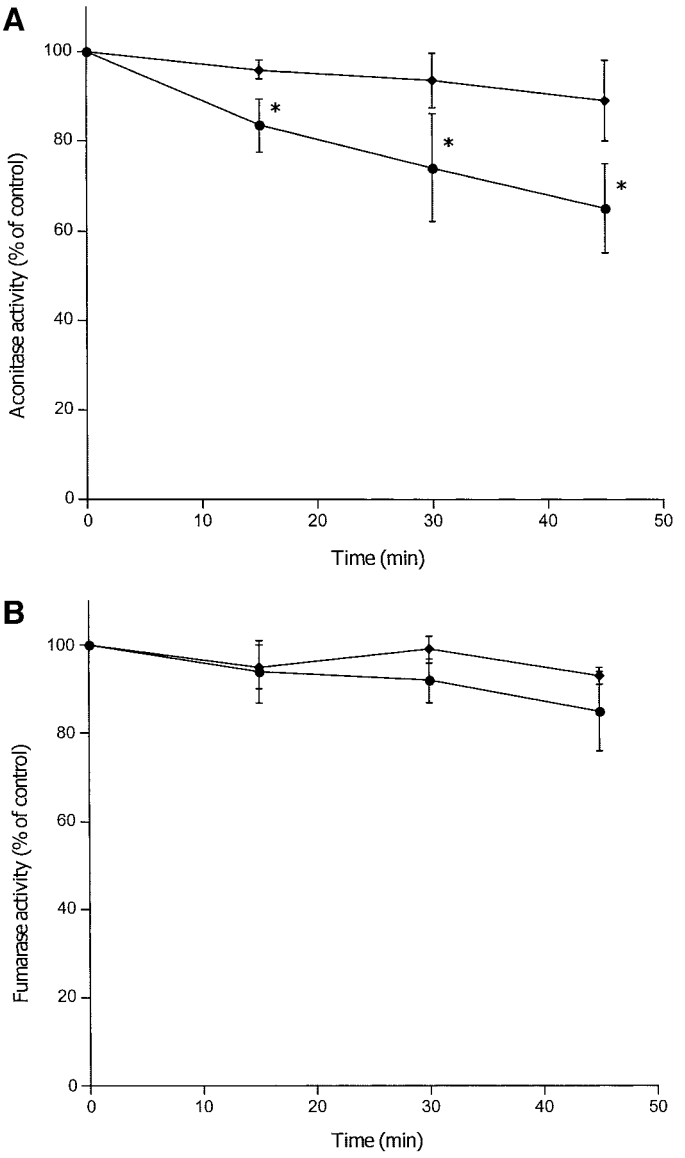

Fig. 7. Effect of GSH depletion on the mitochondrial matrix enzyme activity. Control and GSH depleted mitochondria (90 ± 7%) were incubated with glutamate/malate at 25° in buffer containing 230 mM mannitol, 70 mM sucrose, 20 mM Tris-HCl (pH adjusted to 7.4 with MOPS). At the indicated times, mitochondria were treated with 0.5% Triton X-100, and enzyme activity was measured. A, aconitase activity was assayed in a reaction mixture containing 50 mM Tris-HCl, pH 7.4, 30 mM sodium citrate, 0.6 mM $MnCl_2$, 0.2 mM $NADP^+$, and 1 U/ml of isocitrate dehydrogenase. Isocitrate formation was followed at 340 nm at 25° for 10 min. B, fumarase activity was assayed spectrometrically by monitoring the increase in absorbance at 240 nm at 25°C. The reaction mixture was composed of 30 mM KH_2PO_4, pH 7.4, 0.01 mM ETDA, and 5 mM malate. *, $P < 0.05$ compared with control.

mitochondrial matrix, the activities of two matrix enzymes, aconitase and fumarase, were determined. Aconitase contains an iron-selenium cluster in the catalytic site that makes it very susceptible to inactivation by reactive oxygen species such as H_2O_2 (Nulton-Persson and Szweda, 2001). Fumarase, on the other hand, lacks any distinct features, making it vulnerable to H_2O_2. Incubation of mitochondria with glutamate/malate resulted in a decrease of up to 35% in aconitase activity at 45 min in GSH-depleted mitochondria (90 ± 7%), whereas aconitase of control mitochondria displayed only an 11% decrease (Fig. 7A). As expected, much less decrease in fumarase activity was observed in both control and GSH-depleted mitochondria (Fig. 7B). Control mitochondria exhibited only a 7% decrease in fumarase activity, whereas GSH depleted mitochondria exhibited a 15% decrease.

Discussion

Extensive studies using isolated mitochondria and various inhibitors have identified the flavoprotein component in complex I (Turrens and Boveris, 1980) and ubisemiquinone in complex III (Cadenas et al., 1977; Turrens et al., 1985) as the major sources of $O_2^{\cdot-}$ in the respiratory chain. The stimulatory effects of antimycin, which increases $UQ_O^{\cdot-}$ levels but inhibits $UQ_I^{\cdot-}$ formation (de Vries, 1986), suggests that $UQ_O^{\cdot-}$ not $UQ_I^{\cdot-}$, is important in $O_2^{\cdot-}$ generation by complex III. X-ray crystallography studies have shown that the Qo site in complex III lies near the intermembrane space (Iwata et al., 1998), whereas flavoprotein of NADH dehydrogenase is suspected to be oriented toward the matrix side (Walker, 1992). Thus, mitochondrial topology predicts that complex I generates $O_2^{\cdot-}$ toward the matrix, whereas complex III generates $O_2^{\cdot-}$ toward the intermembrane space. Our results are in agreement with what is predicted by topology of mitochondria. In the presence of complex I substrates, H_2O_2 was observed diffusing from the matrix (caused by $O_2^{\cdot-}$ generation into the matrix which is converted to H_2O_2 by Mn-SOD), and the generation of $O_2^{\cdot-}$ by complex I toward the intermembrane space was not observed. On the other hand, in the presence of either complex I or II substrates, a small $O_2^{\cdot-}$ signal that is enhanced by antimycin is observed, indicating complex III generation of $O_2^{\cdot-}$ into the intermembrane space.

Our findings also shows that $UQ_O^{\cdot-}$ in complex III does releases $O_2^{\cdot-}$ not only toward the intermembrane space but also to the matrix. However, in the presence of antimycin, it is possible other components besides $UQ_O^{\cdot-}$might contribute to $O_2^{\cdot-}$ release into the matrix. Looking at the relative nanomoles of $O_2^{\cdot-}$ (~0.32 nmol/min/mg) and H_2O_2 (~2.4 nmol/min/mg) induced by antimycin treatment in GSH-depleted mitochondria, it seems that most $O_2^{\cdot-}$ is generated toward the matrix rather than the intermembrane space. However, because $O_2^{\cdot-}$ can interact with intermembrane space constituents such as cytochrome *c* before detection by EPR (Han et al., 2003), we are probably underestimating the amount of $O_2^{\cdot-}$ being generated into the intermembrane space. In addition, these values may be misleading if some of the measured H_2O_2 generated after antimycin treatment is formed in the intermembrane space from spontaneous $O_2^{\cdot-}$ dismutation or catalyzed by an intermembrane space Cu,Zn-SOD (intermembrane Cu,Zn-SOD has reported in liver but has never been confirmed in heart mitochondria) (Okado-Matsumoto and Fridovich, 2001; Inarrea, 2002). The topology of $O_2^{\cdot-}$ and H_2O_2 in heart mitochondria based on this and other work is summarized in Fig. 8. The relative percentages of $O_2^{\cdot-}$ generated toward the intermembrane space and into the matrix by $UQ_O^{\cdot-}$ remain an important unresolved question.

Although $UQ_O^{\cdot-}$ is generally considered the major source for $O_2^{\cdot-}$ in complex III, our work with myxothiazol supports other studies suggesting that components other than $UQ_O^{\cdot-}$ in complex III can generate $O_2^{\cdot-}$ into the matrix (Starkov and Fiskum, 2001; Young et al., 2002). Ubisemiquinone at the Q_I site ($UQ_I^{\cdot-}$) and cytochrome *b* are reasonable candidates for $O_2^{\cdot-}$ release into the matrix induced by myxothiazol and merit further investigation (Fig. 10). The iron-selenium clusters in complex III are believe to lie near the intermembrane space and so seem to be less likely candidates for $O_2^{\cdot-}$ production into the matrix, although they cannot be ruled out. Topologically, myxothiazol is a unique complex III inhibitor because it can inhibit $O_2^{\cdot-}$ generation toward the intermembrane space and yet stimulate $O_2^{\cdot-}$ generation into the matrix.

GSH peroxidase is considered the major detoxification system for H_2O_2 in the mitochondrial matrix (Chance et al., 1979; Antunes et al., 2002). Although mitochondrial catalase has been described in heart mitochondria (Nohl and Hegner, 1978; Radi et al., 1991), its activity is extremely low and does not seem to play a significant role in H_2O_2 detoxification (Antunes et al., 2002). Similarly, mitochondrial peroxiredoxins, because of their low rate constant with H_2O_2, cannot compensate for the loss of GSH peroxidase activity in mitochondria (Hofmann et al., 2002). This study provides strong experimental evidence for the importance of mitochondrial GSH levels in modulating H_2O_2 levels in the mitochondrial matrix, which had previously only been hypothesized (Flohe et al., 1976). An interesting aspect of this work was the observation of a threshold effect—a certain level of GSH needed to be depleted before H_2O_2 diffusion from the matrix

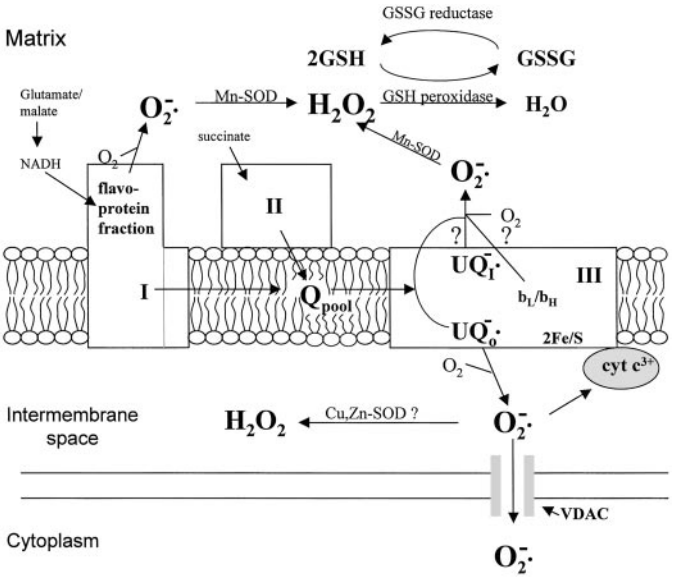

Fig. 8. Scheme showing the topology of superoxide and hydrogen peroxide production by heart mitochondria. Complex I seems to generate $O_2^{\cdot-}$ only toward the matrix, whereas Complex II seems to play no role in $O_2^{\cdot-}$ generation by the electron transport chain. Complex III, on the other hand, generates $O_2^{\cdot-}$ toward both the intermembrane space and the matrix. In presence of antimycin, $Ub_O^{\cdot-}$ seems to generate $O_2^{\cdot-}$ toward both the intermembrane space and the matrix. $Ub_I^{\cdot-}$ and cytochrome *b* are alternative candidates for generation of $O_2^{\cdot-}$ into the matrix, as observed with myxothiazol treatment.

was increased. This observation is in line with the large stoichiometric differences between GSH and H_2O_2 that normally favor detoxification by GSH in the matrix. Small changes in GSH levels are predicted not to affect the catalytic activity of GSH peroxidase because GSH levels are in excess in the matrix. We observed that the GSH-H_2O_2 dose curve with succinate required a slightly lower threshold of GSH depletion (~27%) before H_2O_2 production increased than the threshold observed with glutamate/malate plus rotenone (~37%). This suggests that the rate of H_2O_2 production may determine the GSH depletion threshold, a fact that may have important physiological relevance in vivo.

Disorders such as long-term ethanol intake and cerebral ischemia are associated with decrease in mitochondrial GSH levels of more than 50% (Fernandez-Checa et al., 1987). What are the expected consequences when GSH levels decrease by approximately 50%? Our results show the changes in H_2O_2 production by GSH-depleted mitochondria depend on the level of H_2O_2 generated by mitochondria in vivo. Under normal conditions, H_2O_2 generation by mitochondria is difficult to measure without the aid of inhibitors because basal levels of H_2O_2 production by mitochondria are low. In addition, oxygen tensions in vivo may be up to a magnitude lower than in in vitro system (240 μM in buffer) using isolated mitochondria in which most H_2O_2 measurements are made. Because H_2O_2 generation is linearly related to O_2 tension (Boveris and Chance, 1973), H_2O_2 production in vivo is expected to be lower than measured using isolated mitochondria. At low measured rates of H_2O_2 production (0.02–0.10 nmol/min/mg), we were unable to observe any change in H_2O_2 production in 50% GSH-depleted mitochondria. Thus, under basal conditions, 50% mitochondria GSH depletion is expected to have little or no impact on H_2O_2 diffusion from the mitochondrial matrix.

H_2O_2 production depends on the metabolic state of mitochondria and may become exaggerated under certain conditions. H_2O_2 production may be modulated by NADH levels, substrate levels, and ADP/ATP levels (Boveris and Chance, 1973; Han et al., 2001), and endogenous regulator molecules, such as ceramides, have antimycin like effects; binding to complex III causes increased H_2O_2 production from mitochondria (Garcia-Ruiz et al., 1997). In these conditions of elevated mitochondrial H_2O_2 production that can occur in many pathological conditions, 50% mitochondrial GSH depletion may have profound effects on H_2O_2 diffusion from the matrix in vivo.

It has recently been observed that $O_2^{\cdot-}$ generation by complex I can be enhanced by glutathionylation (Taylor et al., 2003). Thus, GSH/GSSG redox status may modulate H_2O_2 production from complex I. Conversely, the amount of GSSG in the matrix is determined by H_2O_2 levels, along with GSSG reductase activity, $NADP^+$/NADPH status, and GSH concentrations. A complex inter-relationship between GSH levels, GSH redox status, NADP/NADPH status, and H_2O_2 production seems to exist in mitochondria and needs to be further explored. There is no evidence that glutathionylation of complex III can occur. In our work, increased H_2O_2 production from complexes I and III was observed after CDNB treatment, suggesting that changes in GSH levels, not glutathionylation, were responsible for increases in mitochondrial H_2O_2 production.

H_2O_2 and $O_2^{\cdot-}$ released by mitochondria have been implicated in signal transduction, pathophysiology, and aging (Cadenas and Davies, 2000). The present studies have addressed the effect of mitochondrial GSH depletion on mitochondrial H_2O_2 and $O_2^{\cdot-}$ generation. $O_2^{\cdot-}$ release into the intermembrane space by complex III is not influenced by GSH status but H_2O_2 release, which is a result of matrix-directed $O_2^{\cdot-}$ from complex I or III, is greatly influenced by GSH status. Moderate (50%) depletion of matrix GSH amplifies H_2O_2 release when $O_2^{\cdot-}$ directed to the matrix is increased, as may occur in pathological conditions. Moderate depletion of mitochondrial GSH therefore may be of considerable importance in sensitizing cells to disease conditions in which H_2O_2 and $O_2^{\cdot-}$ production are greatly stimulated, such as tumor necrosis factor signaling and effects of sphingolipids. This may contribute to the development of apoptosis or necrosis as well as redox effects on signal transduction.

References

Anderson MF and Sims NR (2002) The effects of focal ischemia and reperfusion on the glutathione content of mitochondria from rat brain subregions. *J Neurochem* **81:**541–549.

Antunes F, Han D, and Cadenas E (2002) Relative contributions of heart mitochondria glutathione peroxidase and catalase to H_2O_2 detoxification in in vivo conditions. *Free Rad Biol Med* **33:**1260–1267.

Boveris A and Cadenas E (1975) Mitochondrial production of superoxide anions and its relationship to the antimycin insensitive respiration. *FEBS Lett* **54:**311–314.

Boveris A and Cadenas E (1997) Cellular sources and steady-state levels of reactive oxygen species, in *Oxygen, Gene Expression and Cellular Function* (Clerch LB and Massaro DJ eds), pp 1–26, Marcel Dekker, New York.

Boveris A and Chance B (1973) The mitochondrial generation of hydrogen peroxide. *Biochem J* **134:**707–716.

Brandt U (1998) The chemistry and mechanics of ubihydroquinone oxidation at center P (Qo) of the cytochrome bc1 complex. *Biochim Biophys Acta* **1365:**261–268.

Cadenas E and Boveris A (1980) Enhancement of hydrogen peroxide formation by protophores and ionophores in antimycin-supplemented mitochondria. *Biochem J* **188:**31–37.

Cadenas E, Boveris A, Ragan CI, and Stoppani AO (1977) Production of superoxide radicals and hydrogen peroxide by NADH- ubiquinone reductase and ubiquinol-cytochrome *c* reductase from beef- heart mitochondria. *Arch Biochem Biophys* **180:**248–257.

Cadenas E and Davies KJ (2000) Mitochondrial free radical generation, oxidative stress and aging. *Free Radic Biol Med* **29:**222–230.

Chance B, Sies H, and Boveris A (1979) Hydroperoxide metabolism in mammalian organs. *Physiol Rev* **59:**527–605.

de Vries S (1986) The pathway of electron transfer in the dimeric QH2: cytochrome *c* oxidoreductase. *J Bioenerg Biomembr* **18:**195–224.

DeLeve LD and Kaplowitz N (1991) Glutathione metabolism and its role in hepatotoxicity. *Pharmacol Ther* **52:**287–305.

Demin OV, Westerhoff HV, and Kholodenko BN (1998) Mathematical modelling of superoxide generation with the bc_1 complex of mitochondria. *Biochemistry (Moscow)* **63:**755–772.

Fernandez-Checa JC, Ooktens M, and Kaplowitz N (1987) Effect of chronic ethanol feeding on rat hepatocytic glutathione. Compartmentation, efflux and response to incubation with ethanol. *J Clin Investig* **80:**57–62.

Finkelstein E, Rosen GM, and Rauckman EJ (1980) Spin trapping. Kinetics of the reaction of superoxide and hydroxyl radicals with nitrones. *J Am Chem Soc* **102:**4994–4999.

Flohe L, Gunzler WA, and Ladenstein R (1976) Glutathione peroxidase, in *Glutathione: Metabolism and Function* (Arias IM and Jakoby WB eds) pp 115–138, Raven Press, New York.

Garcia-Ruiz C, Colell A, Mari M, Morales A, and Fernandez-Checa JC (1997) Direct effect of ceramide on the mitochondrial electron transport chain leads to generation of reactive oxygen species. Role of mitochondrial glutathione. *J Biol Chem* **272:**11369–77.

Garcia-Ruiz C, Colell A, Morales A, Kaplowitz N and Fernandez-Checa JC (1995) Role of oxidative stress generated from the mitochondrial electron transport chain and mitochondrial glutathione status in loss of mitochondrial function and activation of transcription factor nuclear factor-κB: studies with isolated mitochondria and rat hepatocytes. *Mol Pharmacol* **48:**825–834.

Gardner PR and White CW (1995) Application of the aconitase method to the assay of superoxide in the mitochondria matrices of cultured cells: Effects of oxygen, redox-cycling agents, TNF-α, IL-1, LPS and inhibitors of respiration, in *The Oxygen Paradox* (Davies KJA and Ursini F eds), Cleup University Press, Padova.

Han D, Antunes F, Canali R, Rettori D, and Cadenas E (2003) Voltage-dependent anion channels control the release of the superoxide anion from mitochondria to cytosol. *J Biol Chem* **278:**5557–5563.

Han D, Sen CK, Roy S, Kobayashi MS, Tritschler HJ and Packer L (1997) Protection against glutamate-induced cytotoxicity in C6 glial cells by thiol antioxidants. *Am J Physiol* **273:**R1771–R1778.

Han D, Williams E, and Cadenas E (2001) Mitochondrial respiratory chain-dependent generation of superoxide anion and its release into the intermembrane space. *Biochem J* **353:**411–416.

Hansford RG, Hogue BA, and Mildaziene V (1997) Dependence of H_2O_2 formation by

rat heart mitochondria on substrate availability and donor age. *J Bioenerg Biomembr* **29:**89–95.
Harvey PR, Ilson RG, and Strasberg SM (1989) The simultaneous determination of oxidized and reduced glutathiones in liver tissue by ion pairing reverse phase high performance liquid chromatography with a coulometric electrochemical detector. *Clin Chim Acta* **180:**203–212.
Hensley K, Pye QN, Maidt ML, Stewart CA, Robinson KA, Jaffrey F, and Floyd RA (1998) Interaction of α-phenyl-*N*-tert-butyl nitrone and alternative electron acceptors with complex I indicates a substrate reduction site upstream from the rotenone binding site. *J Neurochem* **71:**2549–2557.
Hirano T, Kaplowitz N, Tsukamoto H, Kamimura S, and Fernandez-Checa JC (1992) Hepatic mitochondrial glutathione depletion and progression of experimental alcoholic liver disease in rats. *Hepatology* **16:**1423–1427.
Hofmann B, Hecht HJ, and Flohe L (2002) Peroxiredoxins. *Biol Chem* **383:**347–364.
Hyslop PA and Sklar LA (1984) A quantitative fluorimetric assay for the determination of oxidant production by polymorphonuclear leukocytes: its use in the simultaneous fluorimetric assay of cellular activation processes. *Anal Biochem* **141:**280–286.
Inarrea P (2002) Purification and determination of activity of mitochondrial cyanide-sensitive superoxide dismutase in rat tissue extract. *Methods Enzymol* **349:**106–114.
Iwata S, Lee JW, Okada K, Lee JK, Iwata M, Rasmussen B, Link TA, Ramaswamy S, and Jap B (1998) Complete structure of the 11-subunit bovine mitochondrial cytochrome bc1 complex. *Science (Wash DC)* **281:**64–71.
Jocelyn PC and Cronshaw A (1985) Properties of mitochondria treated with 1-chloro-2,4-dinitrobenzene. *Biochem Pharmacol* **34:**1588–1590.
Nagai H, Matsumaru K, Feng G, and Kaplowitz N (2002) Reduced glutathione depletion causes necrosis and sensitization to tumor necrosis factor-α-induced apoptosis in cultured mouse hepatocytes. *Hepatology* **36:**55–64.
Nigam D, Shukla GS, and Agarwal AK (1999) Glutathione depletion and oxidative damage in mitochondria following exposure to cadmium in rat liver and kidney. *Toxicol Lett* **106:**151–157.
Nohl H and Hegner D (1978) Evidence for the existence of catalase in the matrix space of rat-heart mitochondria. *FEBS Lett* **89:**126–130.
Nulton-Persson AC and Szweda LI (2001) Modulation of mitochondrial function by hydrogen peroxide. *J Biol Chem* **276:**23357–23361.
Okado-Matsumoto A and Fridovich I (2001) Subcellular distribution of superoxide dismutases (SOD) in rat liver: Cu,Zn-SOD in mitochondria. *J Biol Chem* **276:**38388–93.
Radi R, Turrens JF, Chang LY, Bush KM, Crapo JD, and Freeman BA (1991) Detection of catalase in rat heart mitochondria. *J Biol Chem* **266:**22028–34.
Starkov AA and Fiskum G (2001) Myxothiazol induces H_2O_2 production from mitochondrial respiratory chain. *Biochem Biophys Res Commun* **281:**645–650.
Taylor ER, Hurrell F, Shannon RJ, Lin TK, Hirst J, and Murphy MP (2003) Reversible glutathionylation of complex I increases mitochondrial superoxide formation. *J Biol Chem* **278:**19603–10.
Turrens JF, Alexandre A, and Lehninger AL (1985) Ubisemiquinone is the electron donor for superoxide formation by complex III of heart mitochondria. *Arch Biochem Biophys* **237:**408–414.
Turrens JF and Boveris A (1980) Generation of superoxide anion by the NADH dehydrogenase of bovine heart mitochondria. *Biochem J* **191:**421–427.
Uhlig S and Wendel A (1992) The physiological consequences of glutathione variations. *Life Sci* **51:**1083–1094.
Vendemiale G, Guerrieri F, Grattagliano I, Didonna D, Muolo L, and Altomare E (1995) Mitochondrial oxidative phosphorylation and intracellular glutathione compartmentation during liver regeneration. *Hepatology* **21:**1450–1454.
Walker JE (1992) The NADH: ubiquinone oxidoreductase (complex I) of respiratory chains. *Q Rev Biophys* **25:**253–324.
Young TA, Cunningham CC, and Bailey SM (2002) Reactive oxygen species production by the mitochondrial respiratory chain in isolated rat hepatocytes and liver mitochondria: studies with myxothiazol. *Arch Biochem Biophys* **405:**65–72.
Zoccarato F, Cavallini L, Deana R, and Alexandre A (1988) Pathways of hydrogen peroxide generation in guinea pig cerebral cortex mitochondria. *Biochem Biophys Res Commun* **154:**727–734.
Zoccarato F, Cavallini L, Deana R, and Alexandre A (1990) The action of the glutathione transferase substrate, 1-chloro-2,4-dinitrobenzene on synaptosomal glutathione content and the release of hydrogen peroxide. *Arch Biochem Biophys* **282:**244–247.

Address correspondence to: Dr. Derick Han, School of Medicine, University of Southern California, Los Angeles, CA 90089-9121 USA. E-mail: derickh@usc.edu